Environmental Science & Technology

pubs.acs.org/est

Article

Organic Matter from Redoximorphic Soils Accelerates and Sustains Microbial Fe(III) Reduction

Andreas Fritzsche,* Julian Bosch, Michael Sander, Christian Schröder, James M. Byrne, Thomas Ritschel, Prachi Joshi, Markus Maisch, Rainer U. Meckenstock, Andreas Kappler, and Kai U. Totsche

Cite This: *Environ. Sci. Technol.* 2021, 55, 10821−10831

Read Online

ACCESS | Metrics & More | Article Recommendations | Supporting Information

ABSTRACT: Microbial reduction of Fe(III) minerals is a prominent process in redoximorphic soils and is strongly affected by organic matter (OM). We herein determined the rate and extent of microbial reduction of ferrihydrite (Fh) with either adsorbed or coprecipitated OM by *Geobacter sulfurreducens*. We focused on OM-mediated effects on electron uptake and alterations in Fh crystallinity. The OM was obtained from anoxic soil columns (effluent OM, efOM) and included—unlike water-extractable OM—compounds released by microbial activity under anoxic conditions. We found that organic molecules in efOM had generally no or only very low electron-accepting capacity and were incorporated into the Fh aggregates when coprecipitated with Fh. Compared to OM-free Fh, adsorption of efOM to Fh decelerated the microbial Fe(III) reduction by passivating the Fh surface toward electron uptake. In contrast, coprecipitation of Fh with efOM accelerated the microbial reduction, likely because efOM disrupted the Fh structure, as noted by Mössbauer spectroscopy. Additionally, the adsorbed and coprecipitated efOM resulted in a more sustained Fe(III) reduction, potentially because efOM could have effectively scavenged biogenic Fe(II) and prevented the passivation of the Fh surface by the adsorbed Fe(II). Fe(III)−OM coprecipitates forming at anoxic−oxic interfaces are thus likely readily reducible by Fe(III)-reducing bacteria in redoximorphic soils.

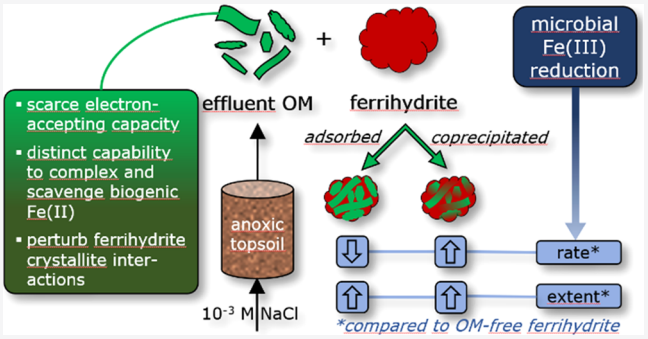

KEYWORDS: *Mössbauer spectroscopy, mediated electrochemical reduction, electron-accepting capacity, ferrihydrite, iron oxide, dissolved organic matter, DOM*

INTRODUCTION

Microbial reduction of poorly soluble Fe(III) to soluble Fe(II) plays an important role in the cycling of iron in circumneutral suboxic and anoxic environments.[1,2] Numerous studies have investigated the factors determining the rate and extent of microbial Fe(III) reduction, with a prominent focus on the impact of natural organic matter (OM). Apart from serving as an energy source and thereby fueling the microbial metabolism,[3−5] previous studies have provided evidence that dissolved natural OM directly affects microbial Fe(III) reduction by acting (i) as a ligand, which increases the solubility of Fe(III),[6] (ii) as a ligand for Fe(II), which helps sustain Fe(III) reduction through the removal of adsorbed Fe(II) from mineral surfaces,[7] (iii) as a redox-active electron-shuttling compound mediating the transfer of electrons from microbial respiration to terminal electron acceptors (iron (oxyhydr-)oxides, dissolved O_2, etc),[8] and (iv) as an adsorbate on Fe(III) mineral surfaces, thereby blocking the access for Fe(III)-reducing bacteria.[9] Natural OM can also indirectly affect the microbial Fe(III) reduction by (v) altering the crystallinity[10] and solubility[11] of iron (oxyhydr-)oxide minerals as well as (vi) their aggregate sizes,[12] which can result in diverse and partially opposing impacts depending on the Fe(III)-reducing bacteria present.[9,13−15]

Many studies have previously confined the impact of natural OM on Fe(III) reduction in soils and sediments to humic isolates from peat, soils, or surface water. Yet, it has been subsequently established that humic substances do not necessarily reflect the properties of OM that is present in soil pore solutions.[16] Hence, approaches that capture the actual solubilization of OM in soils are gaining preference to the use of alkaline extracts, that is, humic substances, as proxies for pedogenic OM.[17] For example, water-extractable OM from organic surface layers was recently used in Fe(III) reduction experiments.[9,18−20] However, it remains unclear if water-extractable OM reflects the composition of OM that occurs in (redoximorphic) soils. Water extractions typically employ (i)

Received: February 19, 2021
Revised: June 30, 2021
Accepted: July 1, 2021
Published: July 21, 2021

https://doi.org/10.1021/acs.est.1c01183
Environ. Sci. Technol. 2021, 55, 10821−10831

liquid-to-solid ratios considerably exceeding those in soils, (ii) agitation, (iii) extraction with ultrapure water, and (iv) predominantly oxic conditions. These conditions are known to preferentially extract certain fractions of OM,[21] for example, compounds with elevated aromaticity,[22] and may also ignore OM fractions relevant for redoximorphic soils. For example, oxic conditions during extraction omit the reductive dissolution of pedogenic iron (oxyhydr-)oxides and thereby the release of OM from the minerals upon their reduction.[23] It has been shown that 72−92% of OM associated with pedogenic iron (oxyhydr-)oxides are not water-extractable;[24] thus, they would not be released by conventional batch water extractions. However, this particular OM represents a likely relevant fraction for microbial Fe(III) reduction in redoximorphic soils. It may migrate through redoximorphic soils eventually encountering anoxic−oxic interfaces where it may (i) coprecipitate with or adsorb to *de novo* Fe(III) minerals[25] and/or (ii) re-oxidize and serve as electron shuttles that accept electrons from microbial respiration.

Our study explores the impact of OM, which was derived from anoxic systems, on microbial Fe(III) reduction. We assessed the rate and extent of microbial reduction by *Geobacter sulfurreducens* of the organomineral ferrihydrite (Fh) with either the adsorbed or coprecipitated OM from an anoxic topsoil. Unlike the water-extractable OM, the OM used in our study includes compounds released by microbial activity under anoxic conditions, for example, OM from the dissolution of pedogenic iron (oxyhydr-)oxides. We focused on the OM-mediated effects on electron transfer and mineral crystallinity rather than the potential of these C sources to serve as e^- donors for microbial Fe(III) reduction. We hypothesize that mobile OM from anoxic topsoil accepts electrons and alters Fh crystallinity, particularly during coprecipitation. We thus expect this anoxic OM to accelerate and sustain microbial Fe(III) reduction.

MATERIALS AND METHODS

Origin of Soil efOM, HA, and Synthesis of Fh. *Effluent Organic Matter.* OM, which is mobile under anoxic conditions, cannot be extracted entirely from intact soils due to the presence of oxic regions, despite, for example, inundation with water.[26] We therefore used a lab-based soil column setup to overcome the limitations of batch extractions with water.[27] All mobile OM eluting from anoxic soil columns is herein referred to as effluent OM (efOM). Air-dried and <2 mm sieved topsoil material (665 ± 25 g; arithmetic mean ± range of two independent soil column replicates) was filled in two replicate soil columns (stainless steel; length: 15.5 cm, diameter: 9.1 cm, V = 1000 cm^3) operated at 295 ± 2 K. The soil material originated from a humus-rich topsoil horizon (Ah; Table S1) of gleyic fluvisol[28] from a floodplain site (Mulde river, Sachsen-Anhalt, Germany). The columns were fed *via* a peristaltic pump (Reglo Analog, Ismatec, Switzerland) with an oxic, low-ionic influent (10^{-3} M NaCl; Merck, Germany; pH ∼ 5.6) at a nominal porewater velocity of 5.5 cm d^{-1} from bottom to top to achieve water-saturated conditions. The average contact time between the liquid and solid phases during percolation was ∼2.8 d. A detailed description of the percolation protocol is provided in Supporting Information S1. Fe(III)- and SO_4^{2-}-reducing conditions were established within the soil columns due to the activity of autochthonous microbial communities and led to the reductive dissolution of pedogenic iron (oxyhydr-)oxides (Figure S1). Upon discharge from the soil column, the effluent solution was exposed to the ambient, oxic atmosphere. At a prevailing effluent pH of ∼7.5 (Figure S1), this would have resulted in the formation of Fe(III)−OM coprecipitates, which form from Fe(II), which is concomitantly present in the soil solution derived from anoxic compartments.[25] Coprecipitation of OM with *de novo* Fe(III) minerals would result in a fractionation between dissolved and mineral-bound OM according to its molecular composition.[29,30] This could be overcome by keeping the soil solution or soil effluent permanently under anoxic conditions until dialysis, that is, the removal of effluent Fe(II) has been completed. To deliver efOM in the required quantities, ∼1.8 L effluent per soil column had to be dialyzed, which required a total of 43 exchanges with ultrapure water (each with ∼10 L). It was therefore unlikely that anoxic conditions could have been maintained during the complete process of dialysis. We therefore chose the following approach to retrieve the entire efOM from anoxic soil: the effluent was acidified with HCl immediately after its discharge from the soil column (final concentration: 0.25 M HCl). The effluent pH remained <1 by this treatment, which effectively retarded the oxidation of the effluent Fe(II).[31] We did not observe any precipitation of OM [*e.g.*, humic acid (HA)]. The acidified effluent was dialyzed to remove coincident Fe(II) and other inorganic ions (100−500 Da, Spectra/Por Biotech CE, Spectrum Laboratories, USA) to prevent the precipitation of iron (oxyhydr-)oxides and of salts during freeze-drying (Alpha 1-4 LSC, Christ, Germany). Although the electric conductivity of the effluent dropped from ∼73 mS cm^{-1} before dialysis (excess H_3O^+ and Cl^-) to ∼40 μS cm^{-1} after dialysis, some Fe remained in the dialyzed effluent most likely as nano-aggregated Fe−OM coprecipitates (Figure S2). With dialysis, the concentration of the effluent Fe decreased from 116 ± 13 to 24 ± 3 mg L^{-1}. Excitation−emission matrices from the corresponding effluent samples indicated that dialysis did not change the composition of efOM except for a potential partial loss in polyphenolic substances (Figure S3). This may have resulted in a dialysis-induced decrease in the electron-donating capacity of efOM. However, this property is irrelevant for our microbial reduction experiments, in which the investigated OM specimens (efOM and HA) did not act as electron donators but rather as potential electron acceptors in microbial reduction. We assumed that the effects on efOM properties by the instant effluent acidification were reversible when the pH was raised to higher values. This assumption was supported by the general reversibility of pH-induced changes in the emission−excitation matrices of efOM (Figure S3 and Table S2). The emission−excitation matrices are sensitive to the changes in OM fluorophores and their molecular environment.[32]

Humic Acid. HA was obtained from anoxic OM-rich groundwater[33] (∼97 mg dissolved OC L^{-1}) from a different site (Gorleben, Germany) by enrichment *via* reverse osmosis and fractionation according to the XAD-8 method.[34] Solid HA was re-dissolved and stirred (1 h) in ultrapure water at pH ∼ 10 (NaOH; Sigma-Aldrich, Germany). Subsequently, the solution pH was re-adjusted to pH = 7 (HCl; Merck), stirred overnight, centrifuged (30 min, 293 K, 10,000 rpm), and filtered (0.22 μm, sterile polyethersulfone, Millex-GP; Merck Millipore; Germany).

Ferrihydrite. 6-Line Fh was synthesized by dissolving 5 g $Fe(NO_3)_3 \times 9H_2O$ (Sigma-Aldrich) in 500 mL of ultrapure water, stirring at 348 K for 12 min, and subsequently cooling down to room temperature in an ice bath (final pH = 5.7).[35]

https://doi.org/10.1021/acs.est.1c01183
Environ. Sci. Technol. 2021, 55, 10821−10831

For coprecipitation with HA, HA solutions with 2.0, 60.5, and 184 mg OC L^{-1} were used instead of water, which correspond to OC/Fe ratios of 0.01, 0.32, and 0.96 mol_C/mol_{Fe}, respectively, in the solutions. For coprecipitation with efOM, 1 g $Fe(NO_3)_3 \times 9H_2O$ was dissolved in 200 mL dialyzed, efOM-containing effluent from the duplicate soil columns (OC = 65 ± 1 mg L^{-1}), resulting in OC/Fe ratios of ~0.44 mol_C/mol_{Fe} in the solutions. For adsorption, OM-free Fh was stirred for 3 d in the dark in HA solutions and in dialyzed soil effluent to obtain OC/Fe ratios of 0.01, 0.32, 0.96 (adsorbed HA), and 0.68 mol_C/mol_{Fe} (adsorbed efOM) in the solutions. With respect to the effluents from anoxic soil columns,[25] these initial OC/Fe ratios were comparably low. This was chosen to prevent the formation of organic Fe(III) complexes, which is reported at higher initial OC/Fe ratios.[36] Organically complexed Fe(III) is distinctly more available for microbial reduction[37] and could therefore mask any effects by OM-mediated alterations in Fh crystallinity and electron shuttling. To remove the residual nitrate from synthesis, all Fh suspensions were dialyzed (6 kDa; ZelluTrans T2, Roth, Germany) against ultrapure water.

Analyses. The electron-accepting capacity (EAC) of HA and efOM, that is, the number of electrons transferred to the redox-active constituents in a given aqueous solution, was quantified by mediated electrochemical reduction.[38] In brief, a 9 mL glassy carbon cylinder served as both the working electrode and the electrochemical reaction vessel. The reduction potential (E_h) applied to the working electrode was referenced against Ag/AgCl reference electrodes (Bioanalytical Systems Inc., USA) but is reported *versus* the standard hydrogen electrode. We used a Pt wire counter electrode in a counter electrode compartment that was separated from the working electrode compartment by a porous glass frit. Both the reference and the counter electrode compartment (filled with 1 mL of 0.1 M KCl, 0.1 M phosphate, pH = 7) were lowered into the glassy carbon cylinder (filled with 5.5 mL of 0.1 M KCl, 0.1 M phosphate, pH = 7). The mediated electrochemical reduction was conducted at E_h = −0.49 V using diquat dibromide monohydrate (99.5%, Supelco, USA; final concentration: 0.231 mM) as the dissolved electron transfer mediator in the cell. The values for the EAC were determined by the integration of the reductive current peaks.[38] As efOM was exposed to the ambient atmosphere after its discharge from the soil column, we propose that it was re-oxidized by O_2 before being assessed with electrochemical mediated reduction.[39,40]

Powder X-ray diffractograms of Fh specimens were obtained from freeze-dried, mortared samples on Si(911) holders (Cu Kα, 40 kV, 40 mA; D8 ADVANCE, Bruker, Germany). ^{57}Fe Mössbauer spectroscopy was conducted at the Center of Applied Geosciences Tübingen (Eberhard-Karls-University, Germany). The spectra of the freeze-dried Fh samples were collected at room temperature (295 K) and 5 K using a closed-cycle cryostat (Janis Research, USA). Selected samples were measured at 70 K, which was identified in a separate test series as an approximate blocking temperature (T_N) of the organomineral 6-line Fh. Mössbauer spectra were recorded in transmission mode using a constant acceleration drive system (Wissel, Germany) with a source of ^{57}Co in a Rh matrix. The spectra were calibrated against the measurement of α-Fe(0) foil at room temperature and were evaluated with the Recoil software package using Voigt-based fitting.[41] For the spectra obtained at room temperature and 5 K, we chose a single-site model with two Gaussian components to reflect the spectral asymmetries in the Mössbauer spectra, except for three samples, where a two-site model was more appropriate (see Results and Discussion). For the spectra obtained at 70 K, we chose a two-site model to reflect the coexistence of a magnetically polarized (sextet) and nonpolarized (doublet) component. Iron in efOM-containing soil effluents was analyzed with inductively coupled plasma with optical emission spectrometry (725-ES, Varian). The contents of C, N, S, O, and H were determined with an elemental analyzer (Euro EA, EuroVector, Italy).

Microorganisms, Media, and Reduction Experiments. *G. sulfurreducens* strain DSMZ 12127[42] was obtained from the German Collection of Microorganisms and Cell Cultures (DSMZ, Braunschweig, Germany). The strain was cultivated using standard anaerobic techniques at 303 K in darkness under a N_2/CO_2 (80/20, v/v) atmosphere. The media composition for cell precultivation, cultivation, and harvesting is specified elsewhere (Table S3). For the reduction experiments, 1.4 mL of concentrated cell suspension was added to 10 mL of low-salt mineral medium with trace elements and selenium−tungsten, which contained 11% of the concentration of each compound compared to the (pre-)cultivation medium (Table S3E−H), 11 μM cAMP, and 3.85 mM Na acetate as the C and energy source. The suspensions were buffered at pH ~ 6.8 (Tris-HCl; Merck). Dialysis of the Fh-containing microbial medium, which was conducted for separate experiments (SpectraPor Biotech CE 20 kDa), revealed that the organic constituents of the microbial medium were not associated with Fh. As opposed to Fh, the organic molecules were completely removed from the dialyzed suspension. Phosphate was omitted in the media for reduction experiments to avoid the precipitation of vivianite. Stock suspensions with OM-free Fh and organomineral Fh were added to achieve 4 mM Fe in each batch. Considering the microbial reduction of 8 mol Fe(III) to oxidize 1 mol acetate,[1] acetate was added in excess in our reduction experiments. All reduction experiments were performed in triplicates. As a positive control, 30 mM Fe(III)-citrate (AppliChem; Germany) was added as an electron acceptor instead of Fh. Negative controls were conducted in the absence either of Na acetate or of *G. sulfurreducens* (0.22 μm filtered cell suspension) and did not show Fe(II) formation (Figure S4). Aqueous Fe(II) was measured in triplicate with the ferrozine assay (560 nm; Wallac 1420 Viktor^3 plate reader, PerkinElmer, USA).[43]

Quantification of Rates and Extents of Microbial Fe(III) Reduction. We applied a pseudo-first-order rate equation (eq 1) to describe the observed nonlinear increase of Fe(II) according to

$$\frac{\partial c(t)}{\partial t} = k \times (c_{MAX} - c(t)) \quad (1)$$

where $c(t)$ is the Fe(II) concentration (mM) at time t (h), k is the rate constant (h^{-1}), and c_{MAX} is the Fe(II) concentration (mM), to which $c(t)$ converged during the reduction experiments. We solved eq 1, assuming $c(t_0) = c_{INIT}$, that is, the Fe(II) concentration at the start of the experiment. c_{INIT}, c_{MAX}, and k were fitted against the measured Fe(II) concentrations using the Levenberg−Marquardt algorithm for local optimization.[44] We calculated the 0.95 confidence interval of each fitted parameter to compute the confidence interval of the predicted Fe(II) concentrations. Assuming that Fe(II) production is exclusively coupled to Fh consumption,

https://doi.org/10.1021/acs.est.1c01183
Environ. Sci. Technol. 2021, 55, 10821−10831

Table 1. Contents of C, N, S, O, H, and Fh and EEACs of HA from Anoxic Groundwater and Soil efOM from an Anoxic Topsoil of a Floodplain Site (Table S1)[a]

sample	C	N	S	O	H	∑	C/N	C/S	Fh[b]	measured EAC		EAC_{OM}[c]
	g kg^{-1}						g g^{-1}		g kg^{-1}	mmol e$^-$ (mol OC)$^{-1}$	mol e$^-$ (mol Fe)$^{-1}$	µmol e$^-$ (g OM)$^{-1}$
HA	537	3.6	16.5[d]	309	44.2	911	149	33		25.6±0.3	124.0±1.6	1134±15
$efOM_A$	302	9.9	14.3[d]	385[e]	47.5[e]	759	31	21	222	*91.1±2.1*	1.01±0.01	27±33
$efOM_B$	339	16.3	16.1[d]	394[e]	47.4[e]	813	21	21	191	*70.5±2.1*	1.02±0.01	42±21

[a] $_{A/B}$: independent replicates. Gray values: normalization to OC concentrations invalid as EAC was dominated by Fe(III). [b]Estimated from the OC/Fe concentration ratios in the corresponding effluents; assumptions: all Fe bound in 2l-Fh and $M_{2l\text{-}Fh}$ = 195.7 g mol^{-1} ($Fe_2O_3 \cdot 2H_2O$).[79] [c]Corrected for contribution of Fe(III) to EAC (assuming Fe_{total} = Fe(III)): EAC_{OM} = (EAC (µmol e$^-$ L^{-1}) − Fe (µmol L^{-1}))/OM (g L^{-1}). [d]Sulfate detected with ion chromatography → subtracted from total S. [e]Includes contributions from the coexistent organomineral Fh.

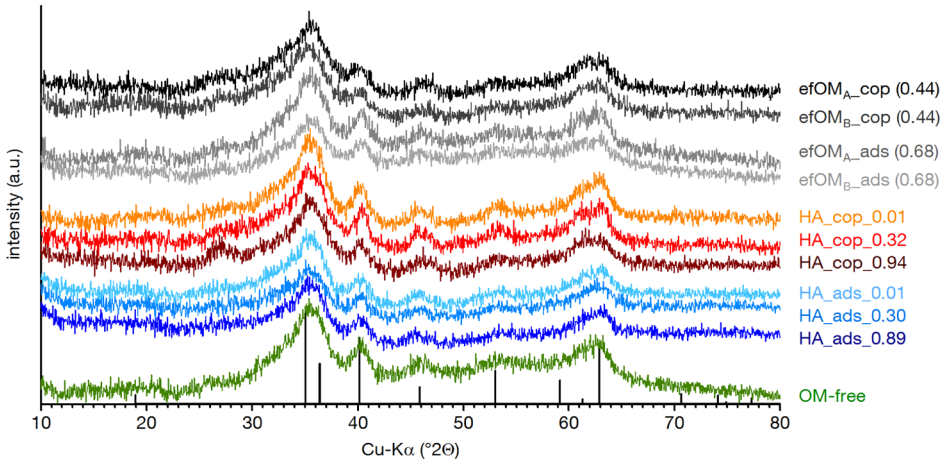

Figure 1. Powder XRD patterns of OM-free Fh and organomineral Fh with adsorbed (ads) and coprecipitated (cop) OM. efOM: soil efOM from an anoxic topsoil of a floodplain site (Table S1). $_{A/B}$: independent replicates. HA: humic acid from anoxic groundwater. The values in the sample name denote the molar OC/Fe ratio, which was set in the corresponding suspension. Black bars depict the powder diffraction reference file of 6-line Fh.[80]

the half-life of Fh ($T_{1/2}$; h) converging to the concentration of residual (nonreducible) Fh was calculated according to eq 2.

$$T_{1/2} = \frac{\ln 2}{k} \tag{2}$$

RESULTS AND DISCUSSION

Properties of efOM from Anoxic Topsoil. HA commonly facilitates the microbial reduction of iron (oxy-hydr-)oxides, but the extent to which these findings apply to redoximorphic soils remains unclear. Compared to HA from anoxic groundwater, efOM from our soil column experiments reproducibly exhibited a very different chemical composition. The combined masses of C, N, S, O, and H accounted for only 79 ± 3% of the mass of efOM, compared to ∼91% of the mass of HA (Table 1). The remaining mass of efOM is attributed to the abundance of residual nano-aggregated Fe−OM coprecipitates (Figure S2). These precipitates contain poorly crystalline Fh[25] probably formed from Fe(II), which resided in the effluent despite dialysis, due to the increase in the effluent pH from 0.9 (acidified with 0.25 M HCl) to 4.8 after dialysis against ultrapure water. Assuming that Fe present in the dialyzed effluent was present as Fh,[25] the mass of Fh must have accounted for 21 ± 2% in efOM (Table 1), thereby closing the gap in efOM mass balance. The C/N ratios were clearly lower in efOM than in HA. Assuming that amides are the dominant chemical forms of nitrogen in the OM from soils and sediments,[17] the relative content of peptides was likely higher in efOM than in HA, which was also revealed by the corresponding ^{13}C NMR spectra (Figure S5). Absorbance bands, characteristic of proteins and polysaccharides, were more pronounced in the Fourier transform infrared spectroscopy (FTIR) spectra of efOM and of organomineral Fh with efOM than in the spectra of HA and HA-associated Fh (Figure S6). efOM also exhibited a comparably low C/S ratio (Table 1). Considering that efOM was mobilized under sulfate-reducing conditions,[26] it is possible that the elevated S content of efOM resulted from the reactions of H_2S with organic molecules.[45,46] As HA was obtained from anoxic groundwater,[33] the C/S ratio was also low in comparison to ancillary OM references, which were retrieved under oxic conditions (*i.e.*, water-extractable OM; Table S4).

The EAC of efOM was dominated by Fe(III) (Table 1), consistent with the complete reduction of Fe(III) in the residual, low-crystalline Fe−OM coprecipitates,[25] as previously demonstrated for Fh.[47] This conclusion was based on a close-to-exact match between the number of electrons accepted by the dialyzed effluents and their molar Fe concentrations (Table 1). We exclude the presence of Fe(II) in the dialyzed effluent because Fe(II) is expected to rapidly oxidize to Fe(III) after exposing the effluent to ambient air.[25] The good agreement between EAC values and molar Fe(III) contents implies that organic molecules in efOM did not significantly contribute to the measured EAC values (EAC_{OM} in Table 1), likely reflecting

https://doi.org/10.1021/acs.est.1c01183
Environ. Sci. Technol. 2021, 55, 10821−10831

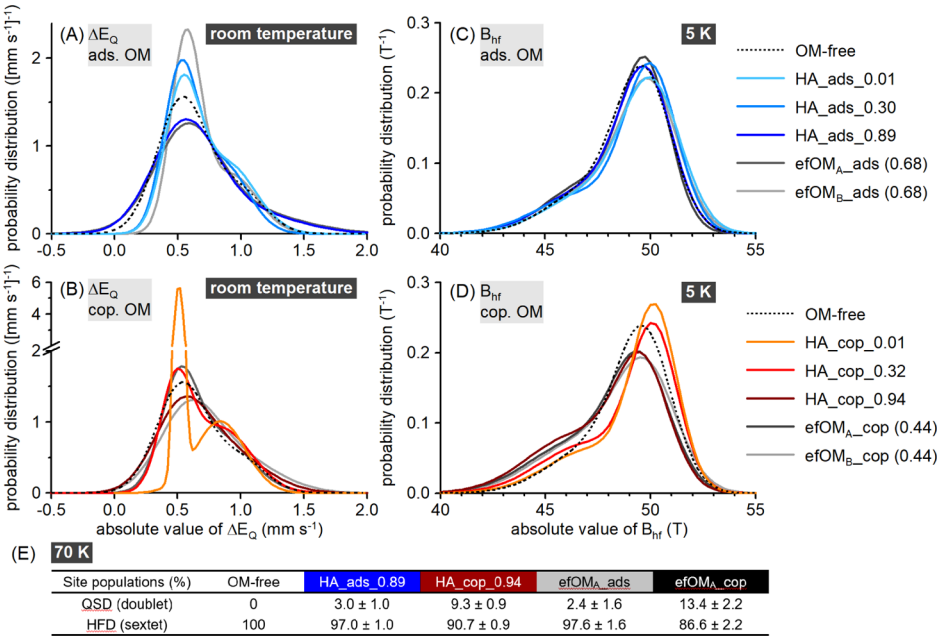

Site populations (%)	OM-free	HA_ads_0.89	HA_cop_0.94	efOM$_A$_ads	efOM$_A$_cop
QSD (doublet)	0	3.0 ± 1.0	9.3 ± 0.9	2.4 ± 1.6	13.4 ± 2.2
HFD (sextet)	100	97.0 ± 1.0	90.7 ± 0.9	97.6 ± 1.6	86.6 ± 2.2

Figure 2. Probability distributions of (A,B) quadrupole splitting (ΔE_Q) and (C,D) of the magnetic hyperfine field (B_{hf}) obtained from the fitted Mössbauer spectra of the OM-free and organomineral Fh's recorded at room temperature and 5 K, respectively. (E) Proportion of the doublet and sextet components required to fit the Mössbauer spectra recorded at 70 K (near the blocking temperature; Figure S7 and Table S5). ads: adsorbed OM. cop: coprecipitated OM. efOM: soil efOM from an anoxic topsoil of a floodplain site (Table S1). $_{A/B}$: independent replicates. HA: humic acid from anoxic groundwater. ±: standard deviation. The values in the sample name denote the molar OC/Fe ratio, which was set in the corresponding suspension.

the absence (or very low concentration) of quinones and other reducible organic moieties in efOM.[48] We evaluated the possibility of the effluent Fe(III) concentration having masked the otherwise detectable contributions of reducible moieties in the efOM to EAC: if the efOM had exhibited an EAC representative of terrestrial HA (1.5 mmol e^- (g OM)$^{-1}$) or of terrestrial fulvic acid (0.8 mmol e^- (g OM)$^{-1}$),[48] these moieties would have increased the measured EAC values by 56 ± 5 or 30 ± 3%, respectively. Such contributions by organic moieties in efOM would have been readily detectable by mediated electrochemical reduction. The absence of OM-mediated EAC was generally reproduced for efOM from an ancillary anoxic topsoil (efOM$_{Ap}$[1] in Table S4). However, the organic molecules in its independent replicate (efOM$_{Ap}$[2]) exhibited a small EAC, which was nevertheless clearly below our (Table S4) and reported EAC values[48,49] for humic substances and batch water extracts from organic surface layers. As opposed to efOM, the EAC values of HA were dominated by organic redox-active moieties (Table 1).

We ascertain that the EAC of humic substances (and water-extractable OM) is significantly higher than the EAC of OM that is likely available at anoxic−oxic interfaces in redoximorphic soils, where electron shuttling might be a particularly important process. Based on the measured EAC values, we would therefore expect increased microbial Fe(III) reduction rates with increasing amounts of HA, while efOM may rather passivate the Fh aggregate surface for electron uptake and thereby slow down Fe(III) reduction.

Effect of efOM on the Mineral Properties of Organomineral Fh. Besides (not) mediating electron transfers, OM may affect the microbial Fe(III) reduction by altering the crystallinity of iron (oxyhydr-)oxides in organomineral associations.[23,49] In our study, the XRD patterns indicated that all syntheses produced 6-line Fh, irrespective of whether they were performed in the absence or presence of HA or efOM (Figure 1). Considering the reflection width, we observed no consistent change in the long-range ordering of the Fh crystallites. FTIR spectroscopy confirmed that all syntheses produced 6-line Fh (Figure S6). HA-characteristic bands increased in the FTIR spectra of Fh−HA (adsorbed/coprecipitated) with increasing initial OC/Fe ratios during the Fh synthesis, consistent with the increasing relative OM contents in these specimens.

Mössbauer spectroscopy revealed (super)paramagnetic iron phases (doublets) at room temperature and magnetically ordered iron phases at 5 K (sextets, Figure S7). The center shifts in the room temperature spectra ranged between 0.33 and 0.36 mm s^{-1} (Table S5), which is in agreement with the presence of Fe(III).[50] The center shifts are within the range of the reported low-crystalline iron (oxyhydr-)oxides, which either reacted with efOM[25] or water-extractable OM[10] or were formed by redox cycles in tropical soils.[51] Moreover, the center shifts did not reveal a consistent trend for Fh associated with HA or efOM *via* adsorption or coprecipitation at variable OM loadings. Two Gaussian components were required to account for the asymmetry in the doublets and sextets, except for three spectra recorded at room temperature (OM-free Fh; Fh with adsorbed HA, and Fh with adsorbed efOM), where an additional component (collapsed sextet) was required to obtain physically meaningful fits (Figure S7 and Table S5). This could indicate an incipient magnetic ordering already at room temperature, which may point to the presence of goethite in these synthesized materials. If so, the relative contribution of goethite would be very low, considering the absence of goethite-specific reflections and bands in the XRD patterns (Figure 1) and FTIR spectra (Figure S6), respectively. The quadrupole splitting (ΔE_Q) contains the most information on the intraparticle atomic order, which can be extracted from

https://doi.org/10.1021/acs.est.1c01183
Environ. Sci. Technol. 2021, 55, 10821−10831

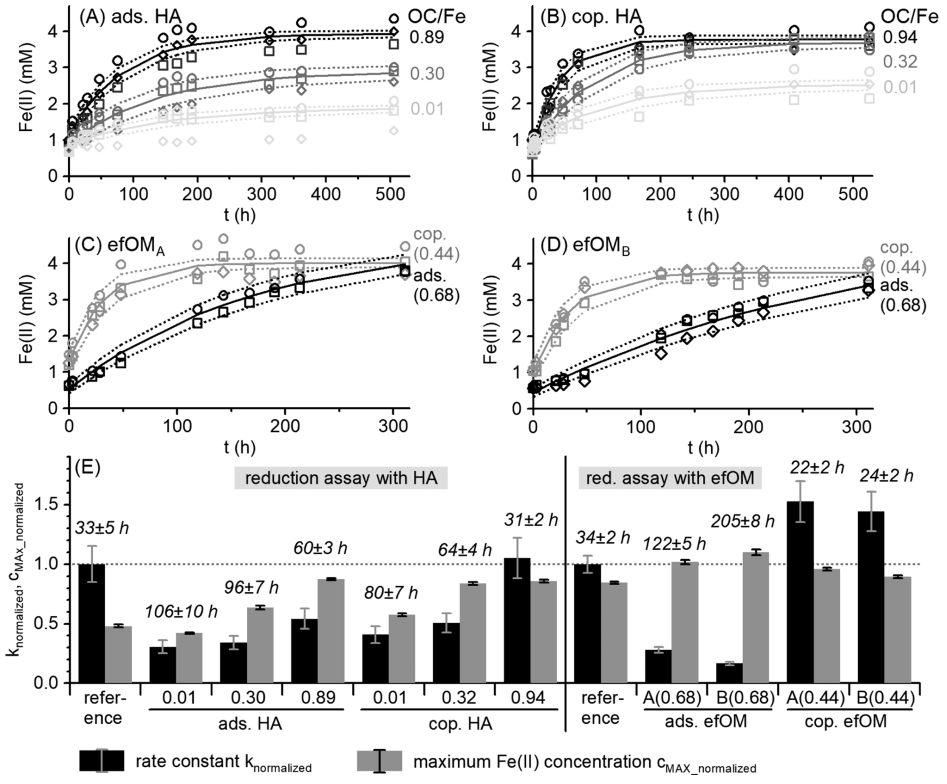

Figure 3. (A–D) Evolution of Fe(II) during the microbial reduction of Fh with adsorbed (ads.) and coprecipitated (cop.) OM. HA: humic acid from anoxic groundwater. efOM: soil efOM from an anoxic topsoil of a floodplain site (Table S1). $_{A/B}$: independent replicates. Symbols depict mean values of three replicate experiments. Solid/dashed lines depict the prediction of mean Fe(II) concentrations and the corresponding 95% confidence intervals, respectively, on the basis of fitted k, c_{MAX}, and c_{INIT} (eq 1). (E) Rate constants ($k_{normalized}$), the corresponding half-life of Fh (*italic values*), and maximum Fe(II) concentrations ($c_{MAX\_normalized}$), which parameterize the observed microbial reduction of OM-free Fh (reference) and organomineral Fh. The values in the sample description denote the molar OC/Fe ratio, which was set in the corresponding suspension. k was normalized to the reduction rate of the corresponding OM-free Fh (reference). c_{MAX} was normalized to the total Fe concentration, which was expected in each treatment [Fe from Fh + *Geobacter* inoculum (Table S3) + residual Fe in efOM (Figure S2)]. Error bars and "±" denote the standard errors.

a Mössbauer spectrum,[52,53] and is influenced by the interactions of iron with other atoms in the mineral lattice.[54] The higher values of ΔE_Q correspond to a higher degree of distortion relative to a perfect polyhedral ligand electric field.[55] Such distortion arises due to the presence of foreign ligands other than O and OH, for example, OM.[10] Although the mean values of ΔE_Q were consistently higher for the organomineral Fh compared to the OM-free Fh, these—contrary to our expectations—were not consistently shifted toward higher values for Fh coprecipitated with increasing amounts of HA (Table S5). The highest mean value of ΔE_Q was observed for Fh coprecipitated with efOM$_B$, which, however, was less pronounced in its independent replicate (efOM$_A$_cop in Table S5). The broad distributions of ΔE_Q were positively skewed with the most probable ΔE_Q of ∼0.6 mm s^{-1} and a strong tailing up to 1.5–2 mm s^{-1}, with no obvious dependence on the type and amount of added OM and the mode of association with Fh (Figure 2A,B). Shifts in ΔE_Q values toward higher values were previously reported when pure iron (oxyhydr-)oxides were treated with stepwise increased concentrations of organic additives.[10,56] Therefore, we infer that Mössbauer spectroscopy is generally capable of detecting such an OM-induced distortion of Fh polyhedra. We therefore expect a similar degree of intraparticle order in all organomineral Fh of this study, independent of the type and amount of added OM, while the Fh polyhedra in OM-free Fh exhibit a higher degree of atomic order. The mean values of magnetic hyperfine fields (B_{hf}), which were derived from Mössbauer spectra recorded at 5 K, shifted systematically to lower B_{hf} and more HA was coprecipitated with Fh. In contrast, no such decrease was observed for Fh with increasing amounts of adsorbed HA (Table S5). A lower B_{hf} at a constant ΔE_Q points to a higher perturbation of crystallite interactions.[57] OM is known to decrease the crystallite interactions due to magnetic dilution.[56,58] Increased contents of such "foreign" species in the iron precipitates will therefore shift the distributions of B_{hf} to lower values. In our study, two components with the same ΔE_Q and δ, but variable B_{hf}, were applied to fit the asymmetric sextets in the 5 K spectra. The obtained B_{hf} distributions were negatively skewed and covered a wide range of 41–53 T. According to our expectations, the coprecipitation of Fh with efOM and HA shifted the B_{hf} distributions to lower values, while this effect was increasingly pronounced with increasing amounts of HA (Figure 2D). In contrast, adsorption of neither efOM nor HA to Fh shifted the B_{hf} distributions considerably (Figure 2C). Consequently, we assume that decreased crystallite interactions in the organomineral Fh coprecipitated with efOM and HA. This is likely due to the arrangement of OM molecules between Fh crystallites throughout the entire organomineral aggregate. Presumably, this was not the case if the OM molecules were associated with Fh aggregate surfaces *via* post-aggregation adsorption. If single mineral phases are

https://doi.org/10.1021/acs.est.1c01183
Environ. Sci. Technol. 2021, 55, 10821–10831

evaluated, the blocking temperature (T_N) is inversely correlated to the content in the impurities[10,59,60] and positively correlated to the primary particle size of this Fe phase.[53] We found that T_N was ~70 K for the organomineral Fh from this study (Figure S7). At this temperature, the contribution of a magnetically nonpolarized component (doublet) was the highest for Fh coprecipitated with efOM and HA, followed by Fh adsorbed with efOM and HA, while OM-free Fh was still fully magnetically ordered (Figures 2E and S7). According to the B_{hf} distributions extracted from the 5 K spectra (Figure 2C,D), this finding was in general agreement with the expected decrease in T_N due to increasing impurities, which had lowered the crystallite interactions, particularly in the Fh−efOM and Fh−HA coprecipitates. However, while the B_{hf} distribution of OM-free Fh (5 K spectra) was nearly identical to those of Fh with adsorbed HA and efOM (Figure 2C), the latter specimens had small but reproducibly detectable contributions of a magnetically nonpolarized component in their 70 K spectra, which was completely absent in OM-free Fh (Figure S7). We cannot therefore exclude that OM also altered the sizes of Fh primary particles (≠aggregates) besides the perturbation of Fh crystallite interactions. If so, the primary particle sizes presumably increased in the following order according to the individual contributions of the doublet component in the 70 K spectra: $Fh\_efOM_{cop} < Fh\_HA_{cop} \ll Fh\_HA_{ads} \sim Fh\_efOM_{ads} \ll$ OM-free Fh.

Considering the inverse relation between the abiotic reduction rates and Fh primary particle size,[61] we would expect a faster reduction of Fh that is coprecipitated with efOM and HA. Contrarily, given the invariable intraparticle atomic order in the organomineral Fh, we would not expect an influence by the OM type (HA *vs* efOM), its relative content, and the mode of association (adsorbed *vs* coprecipitated), on the microbial Fe(III) reduction rates driven by changes in the crystal order of Fh.

Microbial Reduction Experiments. The microbial reduction of OM-free Fh was relatively fast (half-life ~ 33 h), but incomplete, as indicated by the final Fe(II) concentrations that accounted for 50−80% of the total provided Fe(III) (c_{MAX} in Figure 3E). The microbial reduction of Fh with the adsorbed HA and efOM was consistently slower (k in Figure 3E), which agrees with previous studies showing that OM passivated Fh surfaces.[18,62] With the increasing amounts of adsorbed HA, the microbial reduction accelerated to some extent (Figure 3E). This finding can be rationalized by the beneficial effect of electron-transfer shuttling by HA[33] above a certain threshold value.[9,12] It was speculated that *Geobacter* does not use external electron shuttles in natural habitats rich in OM and iron (oxyhydr-)oxides[19] and that external electron shuttling exerts a minor influence on the reduction of Fe−OM associations.[9] Nevertheless, electron shuttling improved the reduction of ferric minerals.[33,63] As revealed by the lack of a substantial EAC, the organic molecules in efOM—as opposed to HA—could not efficiently accept electrons. This finding supports the idea that efOM passivated the Fh surface for electron uptake. As a consequence, the half-lives of Fh with adsorbed efOM were increased by a factor of 4.8 ± 1.2 compared to OM-free Fh, which was clearly higher than the increase observed in treatments with similar amounts of HA added for adsorption to Fh (Figure 3E).

The extent of Fh reduction increased to ~87% of the expected maximum Fe(II) concentration in treatments with the highest addition of HA for adsorption to Fh, which was approximately twice the extent observed for treatments with the lowest addition of HA for adsorption to Fh. If efOM was adsorbed to Fh, complete Fh reduction occurred (Figure 3E). This particular finding contradicts previous studies that reported lower extents of microbial Fe(III) reduction if water-extractable OM and microbial exudates were added to iron (oxyhydr-)oxides.[9] Following the hard−soft Lewis acid−base concept, which can be used to explain the affinity of metal ions to bind to the topsoil OM,[64] we resolve and explain the observed sustained microbial Fe(III) reduction with the specific capability of efOM to form complexes with biogenic Fe(II). The scavenging of (biogenic) Fe(II) is known to extend the Fe(III) mineral reduction by attenuating the Fe(II)-induced passivation of mineral surfaces and microbial cells[7,65] and the Fe(II)-mediated recrystallization of Fh to more stable Fe(III) minerals.[66] Generally, Fe(II) is considered a comparably soft Lewis acid with a low hardness parameter η_A[67] that is effectively complexed by soft Lewis bases. Such soft Lewis bases are organic ligands with N- and S-containing moieties,[68,69] which are particularly prevalent in anoxic peats[70] and have a higher affinity to Fe(II) than O-containing moieties.[69,71] Sulfate-reducing conditions very likely increased the abundance of S-containing moieties in efOM and HA from anoxic groundwater (C/S in Table 1), presumably due to the reaction with H_2S.[45,46] Interestingly, S-containing moieties were less abundant in ancillary OM specimens derived from batch extractions with water (Table S4). Presumably, this water-extractable OM had not encountered distinct anoxic conditions before and during extraction. The complexation of biogenic Fe(II) by HA during microbial Fe(III) reduction is in line with the increasing extents of Fh reduction with increasing amounts of added HA, independent on the mode of its association with Fh (Figure 3E).

The fastest microbial reduction was reproducibly observed for Fh that was coprecipitated with efOM, exceeding the rate constant of OM-free Fh by a factor of 1.48 ± 0.04. Compared to HA at similar initial OC/Fe ratios, the reduction was faster by a factor of ~3. The reduction of Fh coprecipitated with efOM was nearly complete (93 ± 3% of the expected maximum Fe(II) concentration), yet less exhaustive than in the treatments with adsorbed efOM, in which Fe(III) was entirely reduced to Fe(II) (Figure 3E). We attribute the more sustained Fe(III) reduction in the latter treatments to the higher relative concentration of efOM, which likely resulted in a higher total capacity to form complexes with biogenic Fe(II) and thus to sustain the microbial Fe(III) reduction.

Besides OM-mediated electron transfer, changes in iron (oxyhydr-)oxide crystallinity, and scavenging of biogenic Fe(II), OM may also affect the aggregation properties of iron (oxyhydr-)oxides.[72,73] This effect is relevant considering the inverse correlation of Fe(III) reduction by *Geobacter metallireducens vs* aggregate size.[9] Based on the following observations, we could not find such a relation in our study: (i) Initially, OM-free Fh was dispersed and composed of aggregates with sizes mainly <10 nm (Figure S8). However, when exposed to the microbial medium, settling aggregates >1 μm formed, albeit with comparably short half-lives in the reduction experiments (Figure 3E). (ii) The HA−Fh coprecipitates were composed of settling aggregates at all initial OC/Fe ratios but exhibited decreasing half-lives with an increasing relative abundance of HA. (iii) Fh with adsorbed HA (initial OC/Fe = 0.96 mol_C/mol_{Fe}) was partly dispersed

https://doi.org/10.1021/acs.est.1c01183
Environ. Sci. Technol. 2021, 55, 10821−10831

($Fe_{<0.45\ \mu m}/Fe_{TOTAL}$ = 0.18; data from dynamic light scattering: d_{H1} = 56 ± 8 nm and d_{H2} = 684 ± 192 nm) but was nevertheless more slowly reduced than the settling aggregates of HA−Fh coprecipitates. Consequently, we could not define a consistent relationship between the microbial Fe(III) reduction rates and the actual aggregate sizes of (organomineral) Fh.

In summary, mobile OM from anoxic topsoil (efOM) (i) accepts electrons to a much lesser extent than HA from anoxic groundwater and water-extractable OM from batch extractions, (ii) likely strongly binds Fe(II) involving N- and S-containing moieties (like HA from anoxic groundwater), and (iii) is incorporated in Fh aggregates, which possibly decreases the Fh primary particle size if coprecipitated with Fh (like HA). This resulted—among all tested Fh specimens—in the reproducibly fastest, and nearly complete, microbial reduction of Fh coprecipitated with efOM.

ENVIRONMENTAL IMPLICATIONS

As indicated by our study, Fe(III)−OM coprecipitates that form at anoxic−oxic interfaces in soils are likely readily and completely reducible by Fe(III)-reducing bacteria. This results from OM interfering with the Fe mineral crystallinity and likely scavenging the potential surface passivator Fe(II) but not from electron shuttling to the mineral Fe(III). This is attributed to the properties of the likely available OM in these environments, which is comparably rich in N- and S-containing moieties but only has a negligible capacity to accept electrons. An OM-mediated deceleration of microbial Fe(III) reduction is likely to be expected only in cases when this OM accumulates on the surface of iron (oxyhydr-)oxides, a process that passivates the surface for further electron uptake due to an electron nonconducting layer. Generally, pedogenic Fe(III)−OM coprecipitates were found to become quickly and completely reduced,[74] and another work suggests that reducibility is maintained or increased through reduction and oxidation events.[51]

Our work suggests that OM, which is mobile in anoxic soil regions, may contain much fewer electron-accepting moieties than previously studied OM specimens. This finding is restricted to mobile OM and excludes solid-phase OM, which has a composition different from efOM[16] and was previously shown to contain redox-active moieties both in wetlands[75] and freshwater sediments.[76] However, electron shuttling by OM and thus OM-enhanced microbial reduction of mineral Fe(III)[8] relies on mobile electron acceptors in the OM *sensu stricto*. Colloidal iron (oxyhydr-)oxides could principally act as alternative electron shuttles at anoxic−oxic interfaces in redoximorphic soils. However, it was shown that these Fe(III)-rich aggregates can remain colloidally stable if formed in soil effluents outside of soils[25] but are likely to be completely immobilized if precipitated at anoxic−oxic interfaces within soils.[26] Consequently, we propose that neither Fe(III)−OM coprecipitates nor dissolved OM are likely effective electron shuttles in redoximorphic soils due to their immobility or negligible EACs, respectively.

Microbial processing of efOM (*i.e.*, its oxidation) will likely affect its functionality, which was not considered in the experimental design of this study. In our study, acetate was added in excess and was likely preferred over efOM or HA as the carbon and energy source by *G. sulfurreducens* during the incubations.[77] Furthermore, autochthonous microbial communities—unlike *Geobacter*—[6] might produce endogenous electron-shuttling compounds, which could compensate for the lack (or low abundance) of electron-accepting moieties in efOM. Finally, flow and transport processes along variable gradients are prominent in soils and aquifers and tremendously affect the removal of biogenic Fe(II) and therefore increase the extent of microbial iron (oxyhydr-)oxide reduction and associated bacterial growth.[78] The sustaining of the microbial Fe(III) reduction by efOM-mediated Fe(II) complexation might therefore be superimposed by advective flow in natural porous media.

ASSOCIATED CONTENT

Supporting Information

The Supporting Information is available free of charge at https://pubs.acs.org/doi/10.1021/acs.est.1c01183.

Used topsoil material; design of the soil column experiment and the microbial reduction experiments; ^{13}C NMR spectra, FTIR spectra, and XRD patterns of efOM; properties of ancillary OM specimens for comparison purposes; measured Mössbauer spectra and the corresponding fits; and aggregate properties of OM-free Fh (PDF)

AUTHOR INFORMATION

Corresponding Author

Andreas Fritzsche − *Institute of Geosciences, Friedrich-Schiller-University Jena, D-07749 Jena, Germany;* Present Address: Intrapore GmbH, D-45327 Essen, Germany; orcid.org/0000-0001-5371-2691; Phone: +49 3641 948 715; Email: a.fritzsche@uni-jena.de; Fax: +49 3641 948 742

Authors

Julian Bosch − *Institute of Groundwater Ecology, Helmholtz Centre Munich—German Research Center for Environmental Health, D-85764 Neuherberg, Germany;* Present Address: Intrapore GmbH, D-45327 Essen, Germany

Michael Sander − *Department of Environmental Systems Science, Institute of Biogeochemistry and Pollutant Dynamics, Swiss Federal Institute of Technology (ETH) Zurich, CH-8092 Zurich, Switzerland;* orcid.org/0000-0003-3383-2041

Christian Schröder − *Biological and Environmental Sciences, Faculty of Natural Sciences, University of Stirling, FK9 4LA Stirling, U.K.;* orcid.org/0000-0002-7935-6039

James M. Byrne − *Geomicrobiology, Center for Applied Geosciences, University of Tübingen, D-72076 Tübingen, Germany;* Present Address: School of Earth Sciences, Bristol BS8 1RJ, UK.; orcid.org/0000-0002-4399-7336

Thomas Ritschel − *Institute of Geosciences, Friedrich-Schiller-University Jena, D-07749 Jena, Germany;* orcid.org/0000-0002-9922-1107

Prachi Joshi − *Geomicrobiology, Center for Applied Geosciences, University of Tübingen, D-72076 Tübingen, Germany*

Markus Maisch − *Geomicrobiology, Center for Applied Geosciences, University of Tübingen, D-72076 Tübingen, Germany*

Rainer U. Meckenstock − *Institute of Groundwater Ecology, Helmholtz Centre Munich—German Research Center for Environmental Health, D-85764 Neuherberg, Germany;* Present Address: Environmental Microbiology and

Biotechnology, University of Duisburg-Essen, D-45141 Essen, Germany.; orcid.org/0000-0001-7786-9546
Andreas Kappler − *Geomicrobiology, Center for Applied Geosciences, University of Tübingen, D-72076 Tübingen, Germany;* orcid.org/0000-0002-3558-9500
Kai U. Totsche − *Institute of Geosciences, Friedrich-Schiller-University Jena, D-07749 Jena, Germany;* orcid.org/0000-0002-2692-213X

Complete contact information is available at: https://pubs.acs.org/10.1021/acs.est.1c01183

Notes

The authors declare no competing financial interest.

■ ACKNOWLEDGMENTS

We thank K. Eusterhues for providing water-extractable OM and M. Steffens for ^{13}C NMR spectroscopy. We also thank the reviewers for their valuable comments and suggestions.

■ REFERENCES

(1) Lovley, D. R.; Phillips, E. J. P. Novel mode of microbial energy-metabolism—Organic carbon oxidation coupled to dissimilatory reduction of iron or manganese. *Appl. Environ. Microbiol.* **1988**, *54*, 1472−1480.
(2) Weber, K. A.; Achenbach, L. A.; Coates, J. D. Microorganisms pumping iron: anaerobic microbial iron oxidation and reduction. *Nat. Rev. Microbiol.* **2006**, *4*, 752−764.
(3) LaRowe, D. E.; Van Cappellen, P. Degradation of natural organic matter: A thermodynamic analysis. *Geochim. Cosmochim. Acta* **2011**, *75*, 2030−2042.
(4) Chen, C.; Hall, S. J.; Coward, E.; Thompson, A. Iron-mediated organic matter decomposition in humid soils can counteract protection. *Nat. Commun.* **2020**, *11*, 2255.
(5) Boye, K.; Noël, V.; Tfaily, M. M.; Bone, S. E.; Williams, K. H.; Bargar, J. R.; Fendorf, S. Thermodynamically controlled preservation of organic carbon in floodplains. *Nat. Geosci.* **2017**, *10*, 415−419.
(6) Nevin, K. P.; Lovley, D. R. Mechanisms for accessing insoluble Fe(III) oxide during dissimilatory Fe(III) reduction by *Geothrix fermentans*. *Appl. Environ. Microbiol.* **2002**, *68*, 2294−2299.
(7) Roden, E. E.; Urrutia, M. M. Ferrous iron removal promotes microbial reduction of crystalline iron(III) oxides. *Environ. Sci. Technol.* **1999**, *33*, 1847−1853.
(8) Lovley, D. R.; Coates, J. D.; Blunt-Harris, E. L.; Phillips, E. J. P.; Woodward, J. C. Humic substances as electron acceptors for microbial respiration. *Nature* **1996**, *382*, 445.
(9) Poggenburg, C.; Mikutta, R.; Schippers, A.; Dohrmann, R.; Guggenberger, G. Impact of natural organic matter coatings on the microbial reduction of iron oxides. *Geochim. Cosmochim. Acta* **2018**, *224*, 223−248.
(10) Eusterhues, K.; Wagner, F. E.; Häusler, W.; Hanzlik, M.; Knicker, H.; Totsche, K. U.; Kögel-Knabner, I.; Schwertmann, U. Characterization of ferrihydrite-soil organic matter coprecipitates by X-ray diffraction and Mössbauer spectroscopy. *Environ. Sci. Technol.* **2008**, *42*, 7891−7897.
(11) Mikutta, C.; Kretzschmar, R. Synthetic coprecipitates of exopolysaccharides and ferrihydrite. Part II: Siderophore-promoted dissolution. *Geochim. Cosmochim. Acta* **2008**, *72*, 1128−1142.
(12) Amstaetter, K.; Borch, T.; Kappler, A. Influence of humic acid imposed changes of ferrihydrite aggregation on microbial Fe(III) reduction. *Geochim. Cosmochim. Acta* **2012**, *85*, 326−341.
(13) Cutting, R. S.; Coker, V. S.; Fellowes, J. W.; Lloyd, J. R.; Vaughan, D. J. Mineralogical and morphological constraints on the reduction of Fe(III) minerals by *Geobacter sulfurreducens*. *Geochim. Cosmochim. Acta* **2009**, *73*, 4004−4022.
(14) Bonneville, S.; Van Cappellen, P.; Behrends, T. Microbial reduction of iron(III) oxyhydroxides: effects of mineral solubility and availability. *Chem. Geol.* **2004**, *212*, 255−268.
(15) Bosch, J.; Heister, K.; Hofmann, T.; Meckenstock, R. U. Nanosized iron oxide colloids strongly enhance microbial iron reduction. *Appl. Environ. Microbiol.* **2010**, *76*, 184−189.
(16) Kleber, M.; Johnson, M. G. Advances in understanding the molecular structure of soil organic matter: Implications for interactions in the environment. In *Advances in Agronomy*; Sparks, D. L., Ed.; Academic Press: San Diego, 2010; Vol. *106*, pp 77−142.
(17) Lehmann, J.; Kleber, M. The contentious nature of soil organic matter. *Nature* **2015**, *528*, 60−68.
(18) Eusterhues, K.; Hädrich, A.; Neidhardt, J.; Küsel, K.; Keller, T. F.; Jandt, K. D.; Totsche, K. U. Reduction of ferrihydrite with adsorbed and coprecipitated organic matter: microbial reduction by Geobacter bremensis vs. abiotic reduction by Na-dithionite. *Biogeosciences* **2014**, *11*, 4953−4966.
(19) Cooper, R. E.; Eusterhues, K.; Wegner, C.-E.; Totsche, K. U.; Küsel, K. Ferrihydrite-associated organic matter (OM) stimulates reduction by Shewanella oneidensis MR-1 and a complex microbial consortia. *Biogeosciences* **2017**, *14*, 5171−5188.
(20) Poggenburg, C.; Mikutta, R.; Sander, M.; Schippers, A.; Marchanka, A.; Dohrmann, R.; Guggenberger, G. Microbial reduction of ferrihydrite-organic matter coprecipitates by *Shewanella putrefaciens* and *Geobacter metallireducens* in comparison to mediated electrochemical reduction. *Chem. Geol.* **2016**, *447*, 133−147.
(21) Zsolnay, Á. Dissolved organic matter: artefacts, definitions, and functions. *Geoderma* **2003**, *113*, 187−209.
(22) Rennert, T.; Gockel, K. F.; Mansfeldt, T. Extraction of water-soluble organic matter from mineral horizons of forest soils. *J. Plant Nutr. Soil Sci.* **2007**, *170*, 514−521.
(23) Chen, C.; Meile, C.; Wilmoth, J.; Barcellos, D.; Thompson, A. Influence of pO(2) on iron redox cycling and anaerobic organic carbon mineralization in a humid tropical forest soil. *Environ. Sci. Technol.* **2018**, *52*, 7709−7719.
(24) Gu, B.; Schmitt, J.; Chen, Z.; Liang, L.; McCarthy, J. F. Adsorption and desorption of natural organic matter on iron oxide: mechanisms and models. *Environ. Sci. Technol.* **1994**, *28*, 38−46.
(25) Fritzsche, A.; Schröder, C.; Wieczorek, A. K.; Händel, M.; Ritschel, T.; Totsche, K. U. Structure and composition of Fe-OM co-precipitates that form in soil-derived solutions. *Geochim. Cosmochim. Acta* **2015**, *169*, 167−183.
(26) Fritzsche, A.; Pagels, B.; Totsche, K. U. The composition of mobile matter in a floodplain topsoil: A comparative study with soil columns and field lysimeters. *J. Plant Nutr. Soil Sci.* **2016**, *179*, 18−28.
(27) Wehrer, M.; Totsche, K. U. Detection of non-equilibrium contaminant release in soil columns: Delineation of experimental conditions by numerical simulations. *J. Plant Nutr. Soil Sci.* **2003**, *166*, 475−483.
(28) IUSS Working Group WRB. *World Reference Base for Soil Resources 2014, Update 2015, International Soil Classification System for Naming Soils and Creating Legends for Soil Maps*; FAO: Rome, Italy, 2015.
(29) Eusterhues, K.; Rennert, T.; Knicker, H.; Kögel-Knabner, I.; Totsche, K. U.; Schwertmann, U. Fractionation of organic matter due to reaction with ferrihydrite: Coprecipitation versus adsorption. *Environ. Sci. Technol.* **2011**, *45*, 527−533.
(30) Kalbitz, K.; Solinger, S.; Park, J.-H.; Michalzik, B.; Matzner, E. Controls on the dynamics of dissolved organic matter in soils: A review. *Soil Sci.* **2000**, *165*, 277−304.
(31) Singer, P. C.; Stumm, W. Acidic mine drainage. Rate-determining step. *Science* **1970**, *167*, 1121−1123.
(32) Borisover, M.; Lordian, A.; Levy, G. J. Water-extractable soil organic matter characterization by chromophoric indicators: Effects of soil type and irrigation water quality. *Geoderma* **2012**, *179*−*180*, 28−37.
(33) Wolf, M.; Kappler, A.; Jiang, J.; Meckenstock, R. U. Effects of humic substances and quinones at low concentrations on ferrihydrite

reduction by *Geobacter metallireducens*. *Environ. Sci. Technol.* **2009**, *43*, 5679−5685.
(34) Aiken, G. R.; Thurman, E. M.; Malcolm, R. L.; Walton, H. F. Comparison of XAD macroporous resins for the concentration of fulvic acid from aqueous solution. *Anal. Chem.* **1979**, *51*, 1799−1803.
(35) Schwertmann, U.; Cornell, R. M. *Iron Oxides in the Laboratory*, 2nd ed.; Wiley-VCH Verlag GmbH: Weinheim, Germany, 2000.
(36) Chen, C.; Dynes, J. J.; Wang, J.; Sparks, D. L. Properties of Fe-organic matter associations via coprecipitation versus adsorption. *Environ. Sci. Technol.* **2014**, *48*, 13751−13759.
(37) Braunschweig, J.; Klier, C.; Schröder, C.; Händel, M.; Bosch, J.; Totsche, K. U.; Meckenstock, R. U. Citrate influences microbial Fe hydroxide reduction via a dissolution-disaggregation mechanism. *Geochim. Cosmochim. Acta* **2014**, *139*, 434−446.
(38) Klüpfel, L.; Keiluweit, M.; Kleber, M.; Sander, M. Redox properties of plant biomass-derived black carbon (biochar). *Environ. Sci. Technol.* **2014**, *48*, 5601−5611.
(39) Bauer, I.; Kappler, A. Rates and extent of reduction of Fe(III) compounds and O_2 by humic substances. *Environ. Sci. Technol.* **2009**, *43*, 4902−4908.
(40) Klüpfel, L.; Piepenbrock, A.; Kappler, A.; Sander, M. Humic substances as fully regenerable electron acceptors in recurrently anoxic environments. *Nat. Geosci.* **2014**, *7*, 195−200.
(41) Rancourt, D. G.; Ping, J. Y. Voigt-based methods for arbitrary-shape static hyperfine parameter distributions in Mössbauer spectroscopy. *Nucl. Instrum. Methods Phys. Res., Sect. B* **1991**, *58*, 85−97.
(42) Caccavo, F.; Lonergan, D. J.; Lovley, D. R.; Davis, M.; Stolz, J. F.; McInerney, M. J. Geobacter sulfurreducens sp. nov., a hydrogen- and acetate-oxidizing dissimilatory metal-reducing microorganism. *Appl. Environ. Microbiol.* **1994**, *60*, 3752−3759.
(43) Stookey, L. L. Ferrozine—a new spectrophotometric reagent for iron. *Anal. Chem.* **1970**, *42*, 779−781.
(44) Marquardt, D. W. An algorithm for least-squares estimation of nonlinear parameters. *SIAM J. Appl. Math.* **1963**, *11*, 431−441.
(45) Casagrande, D. J.; Idowu, G.; Friedman, A.; Rickert, P.; Siefert, K.; Schlenz, D. H_2S incorporation in coal precursors: origins of organic sulphur in coal. *Nature* **1979**, *282*, 599−600.
(46) Urban, N. R.; Bayley, S. E.; Eisenreich, S. J. Export of dissolved organic carbon and acidity from peatlands. *Water Resour. Res.* **1989**, *25*, 1619−1628.
(47) Aeppli, M.; Voegelin, A.; Gorski, C. A.; Hofstetter, T. B.; Sander, M. Mediated electrochemical reduction of iron (oxyhydr-)oxides under defined thermodynamic boundary conditions. *Environ. Sci. Technol.* **2018**, *52*, 560−570.
(48) Aeschbacher, M.; Graf, C.; Schwarzenbach, R. P.; Sander, M. Antioxidant properties of humic substances. *Environ. Sci. Technol.* **2012**, *46*, 4916−4925.
(49) Piepenbrock, A.; Schröder, C.; Kappler, A. Electron transfer from humic substances to biogenic and abiogenic Fe(III) oxyhydroxide minerals. *Environ. Sci. Technol.* **2014**, *48*, 1656−1664.
(50) Gütlich, P.; Schröder, C. Mössbauer Spectroscopy. In *Methods in Physical Chemistry*; Schäfer, R., Schmidt, P. C., Eds.; Wiley-VCH: Weinheim, 2012, pp 351−389.
(51) Ginn, B.; Meile, C.; Wilmoth, J.; Tang, Y.; Thompson, A. Rapid iron reduction rates are stimulated by high-amplitude redox fluctuations in a tropical forest soil. *Environ. Sci. Technol.* **2017**, *51*, 3250−3259.
(52) Rancourt, D. G.; Fortin, D.; Pichler, T.; Thibault, P.-J.; Lamarche, G.; Morris, R. V.; Mercier, P. H. J. Mineralogy of a natural As-rich hydrous ferric oxide coprecipitate formed by mixing of hydrothermal fluid and seawater: Implications regarding surface complexation and color banding in ferrihydrite deposits. *Am. Mineral.* **2001**, *86*, 834−851.
(53) Rancourt, D. G.; Thibault, P.-J.; Mavrocordatos, D.; Lamarche, G. Hydrous ferric oxide precipitation in the presence of nonmetabolizing bacteria: Constraints on the mechanism of a biotic effect. *Geochim. Cosmochim. Acta* **2005**, *69*, 553−577.
(54) Rancourt, D. G. Mössbauer spectroscopy in clay science. *Hyperfine Interact.* **1998**, *117*, 3−38.
(55) Rea, B. A.; Davis, J. A.; Waychunas, G. A. Studies of the Reactivity of the Ferrihydrite Surface by Iron Isotopic Exchange and Mössbauer Spectroscopy. *Clays Clay Miner.* **1994**, *42*, 23−34.
(56) Mikutta, C.; Mikutta, R.; Bonneville, S.; Wagner, F.; Voegelin, A.; Christl, I.; Kretzschmar, R. Synthetic coprecipitates of exopolysaccharides and ferrihydrite. Part I: Characterization. *Geochim. Cosmochim. Acta* **2008**, *72*, 1111−1127.
(57) Mørup, S.; Ostenfeld, C. W. On the use of Mössbauer spectroscopy for characterisation of iron oxides and oxyhydroxides in soils. *Hyperfine Interact.* **2001**, *136*, 125−131.
(58) Cornell, R. M.; Schwertmann, U. *The Iron Oxides*, 2nd ed.; Wiley-VCH: Weinheim, Germany, 2003.
(59) Murad, E. Properties and Behavior of Iron Oxides as Determined by Mössbauer Spectroscopy. In *Iron in Soils and Clay Minerals*; Stucki, J. W., Goodman, B. A., Schwertmann, U., Eds.; Springer Netherlands: Dordrecht, 1988, pp 309−350.
(60) Murad, E.; Schwertmann, U. The influence of aluminium substitution and crystallinity on the Mössbauer spectra of goethite. *Clay Miner.* **1983**, *18*, 301−312.
(61) Anschutz, A. J.; Penn, R. L. Reduction of crystalline iron(III) oxyhydroxides using hydroquinone: Influence of phase and particle size. *Geochem. Trans.* **2005**, *6*, 60−66.
(62) Swindle, A. L.; Madden, A. S. E.; Cozzarelli, I. M.; Benamara, M. Size-dependent reactivity of magnetite nanoparticles: A field-laboratory comparison. *Environ. Sci. Technol.* **2014**, *48*, 11413−11420.
(63) MacDonald, L. H.; Moon, H. S.; Jaffé, P. R. The role of biomass, electron shuttles, and ferrous iron in the kinetics of *Geobacter sulfurreducens*-mediated ferrihydrite reduction. *Water Res.* **2011**, *45*, 1049−1062.
(64) Stark, P. C.; Rayson, G. D. Comparisons of metal-ion binding to immobilized biogenic materials in a flowing system. *Adv. Environ. Res.* **2000**, *4*, 113−122.
(65) Royer, R. A.; Burgos, W. D.; Fisher, A. S.; Unz, R. F.; Dempsey, B. A. Enhancement of biological reduction of hematite by electron shuttling and Fe(II) complexation. *Environ. Sci. Technol.* **2002**, *36*, 1939−1946.
(66) Aeppli, M.; Kaegi, R.; Kretzschmar, R.; Voegelin, A.; Hofstetter, T. B.; Sander, M. Electrochemical analysis of changes in iron oxide reducibility during abiotic ferrihydrite transformation into goethite and magnetite. *Environ. Sci. Technol.* **2019**, *53*, 3568−3578.
(67) Parr, R. G.; Pearson, R. G. Absolute hardness: companion parameter to absolute electronegativity. *J. Am. Chem. Soc.* **1983**, *105*, 7512−7516.
(68) Pullin, M. J.; Anthony, C.; Maurice, P. A. Effects of iron on the molecular weight distribution, light absorption, and fluorescence properties of natural organic matter. *Environ. Eng. Sci.* **2007**, *24*, 987−997.
(69) Harris, W. R. Iron Chemistry. *Molecular and Cellular Iron Transport*; Templeton, D. M., Ed.; Marcel Dekker, Inc.: New York, 2005, pp 1−40.
(70) Bhattacharyya, A.; Schmidt, M. P.; Stavitski, E.; Martínez, C. E. Iron speciation in peats: Chemical and spectroscopic evidence for the co-occurrence of ferric and ferrous iron in organic complexes and mineral precipitates. *Org. Geochem.* **2018**, *115*, 124−137.
(71) Jones, A. M.; Collins, R. N.; Rose, J.; Waite, T. D. The effect of silica and natural organic matter on the Fe(II)-catalysed transformation and reactivity of Fe(III) minerals. *Geochim. Cosmochim. Acta* **2009**, *73*, 4409−4422.
(72) Narvekar, S. P.; Ritschel, T.; Totsche, K. U. Colloidal stability and mobility of extracellular polymeric substance amended hematite nanoparticles. *Vadose Zone J.* **2017**, *16*. DOI: 10.2136/vzj2017.03.0063.
(73) Guhra, T.; Ritschel, T.; Totsche, K. U. Formation of mineral-mineral and organo-mineral composite building units from micro-aggregate-forming materials including microbially produced extracellular polymeric substances. *Eur. J. Soil Sci.* **2019**, *70*, 604−615.
(74) Fritzsche, A.; Bosch, J.; Rennert, T.; Heister, K.; Braunschweig, J.; Meckenstock, R. U.; Totsche, K. U. Fast microbial reduction of

ferrihydrite colloids from a soil effluent. *Geochim. Cosmochim. Acta* **2012**, *77*, 444−456.
(75) Roden, E. E.; Kappler, A.; Bauer, I.; Jiang, J.; Paul, A.; Stoesser, R.; Konishi, H.; Xu, H. Extracellular electron transfer through microbial reduction of solid-phase humic substances. *Nat. Geosci.* **2010**, *3*, 417−421.
(76) Lau, M. P.; Sander, M.; Gelbrecht, J.; Hupfer, M. Solid phases as important electron acceptors in freshwater organic sediments. *Biogeochemistry* **2015**, *123*, 49−61.
(77) Glodowska, M.; Stopelli, E.; Schneider, M.; Lightfoot, A.; Rathi, B.; Straub, D.; Patzner, M.; Duyen, V. T.; Berg, M.; Kleindienst, S.; Kappler, A. Role of in Situ Natural Organic Matter in Mobilizing As during Microbial Reduction of FeIII-Mineral-Bearing Aquifer Sediments from Hanoi (Vietnam). *Environ. Sci. Technol.* **2020**, *54*, 4149−4159.
(78) Roden, E. E.; Urrutia, M. M.; Mann, C. J. Bacterial reductive dissolution of crystalline Fe(III) oxide in continuous-flow column reactors. *Appl. Environ. Microbiol.* **2000**, *66*, 1062−1065.
(79) Michel, F. M.; Ehm, L.; Liu, G.; Han, W. Q.; Antao, S. M.; Chupas, P. J.; Lee, P. L.; Knorr, K.; Eulert, H.; Kim, J.; Grey, C. P.; Celestian, A. J.; Gillow, J.; Schoonen, M. A. A.; Strongin, D. R.; Parise, J. B. Similarities in 2-and 6-line ferrihydrite based on pair distribution function analysis of X-ray total scattering. *Chem. Mater.* **2007**, *19*, 1489−1496.
(80) Downs, R. T.; Hall-Wallace, M. The American Mineralogist crystal structure database. *Am. Mineral.* **2003**, *88*, 247−250.

https://doi.org/10.1021/acs.est.1c01183
Environ. Sci. Technol. 2021, 55, 10821−10831